*Computers, Materials & Continua* CMC, vol.65, no.2, pp.1349-1360, 2020

# Fast Compass Alignment for Strapdown Inertial Navigation System

**Jin Sun[1], Dengyin Zhang[1, *], Xiaoye Shi[1] and Fei Ding[1, 2]**

**Abstract:** Initial alignment is the precondition for strapdown inertial navigation system (SINS) to navigate. Its two important indexes are accuracy and rapidity, the accuracy of the initial alignment is directly related to the working accuracy of SINS, but in self-alignment, the two indexes are often contradictory. In view of the limitations of conventional data processing algorithms, a novel method of compass alignment based on stored data and repeated navigation calculation for SINS is proposed. By means of data storage, the same data is used in different stages of the initial alignment, which is beneficial to shorten the initial alignment time and improve the alignment accuracy. In order to verify the correctness of the compass algorithm based on stored data and repeated navigation calculation, the simulation experiment was done. In summary, when the computer performance is sufficiently high, the compass alignment method based on the stored data and the forward and reverse navigation calculation can effectively improve the alignment speed and improve the alignment accuracy.

**Keywords:** Strapdown Inertial Navigation System (SINS), compass alignment, data storage, reverse navigation calculation, forward navigation calculation.

## 1 Introduction

The basic principle of the SINS is to calculate the velocity and position by the integral operation according to the measured acceleration of carrier [Qin (2014); Wang, Zhang, Tong et al. (2020)]. Therefore, the initial alignment must be carried out before the SINS starts operation, so that make the SINS set up an accurate navigation coordinate system. The accuracy of the initial alignment is directly related to the working accuracy of SINS. The initial alignment is one of the key technologies of SINS. Compass alignment method, which is as a mature method originating from the platform INS, is now widely adopted.

As early as 1961, Cannon analyzed the mainstream scheme of the compass alignment method and pointed out that the alignment accuracy and the alignment speed in the compass method is an eternal contradiction. In order to shorten the alignment time, there are many solutions proposed from the perspective of control. For example, the

[1] School of Internet of Things, Nanjing University of Posts and Telecommunication, Nanjing, 21003, China.

[2] Department of Electronic and Electrical Engineering, University College London, London, WC1E 6BT, UK.

[*] Corresponding Author: Dengyin Zhang. Email: zhangdy@njupt.edu.cn.

Received: 09 May 2020; Accepted: 06 June 2020.

segmentation parameter method sets different compass loop parameters in different alignment stages to suppress the oscillation and shorten the convergence time, thereby accelerating the alignment speed. However, these methods do not fundamentally change the accumulation process of the errors, and thus the improvement effect is limited.

The compass self-alignment of SINS on swing base was discussed, and the fine alignment parameters of horizontal and azimuth and the parameter analysis system based on Matlab/Simulink were designed in Li et al. [Li, Xu and Wu (2008)]. Hao et al. [Hao, Zhang and Sun (2011)] studied the compass alignment of large azimuth misalignment. Then the compass alignment method on the basis of time-varying parameters was proposed. Through analyzing the compass alignment process of SINS, a fast compass alignment method for SINS based on saved data and repeated navigation solution was proposed [Liu, Xu, Wang et al. (2013); Chang, Qin and Li (2015)]. A compass method for SINS alignment on moving base is put forward by introducing external reference velocity and designing the setting laws for control-loop parameters in different motion modes [Li, Wu, Wang et al. (2012)]. Aiming at the influence of parameters in compass alignment, taking advantages of genetic algorithm (GA) of global searching, parallel computing and robustness, a GA based compass alignment approach was proposed [Liu, Xu, Zhang et al. (2015)]. In view of the limitations of conventional data processing algorithms, a novel method of compass alignment for SINS is proposed. By means of data storage, the same data is used in different stages of the initial alignment, which is beneficial to shorten the initial alignment time.

The outline of this paper is as follows: Section 1 is the introduction; the compass alignment based on reverse navigation technology is proposed in Section 2; Section 3, and Section 4 respectively verifies the correctness of the algorithm by simulation experiment and triaxial turntable experiment; and Section 5 concludes.

## 2 Compass alignment based on reverse navigation technology

The sampling data of the gyro and accelerometer in the SINS can be regarded as a time series [Chang, Hu and Li (2015); Ren, Liu, Ji et al. (2018)]. In the normal sense, the navigation calculation is to process the sequence in real time and chronological order without data storage, then the real-time navigation results are obtained. If the storage capacity of the navigation computer is large enough and the computing power is strong enough, the sampled data is stored. Since it can be processed in chronological forward direction, it is easy to associate that it can be reversely analyzed and processed. In some cases, when there is no real-time requirement, the forward and reverse repeated analysis on the stored sampled data may improve the alignment accuracy. Perhaps the length of the data actually used for analysis in a certain task is reduced, namely, shorten mission time.

### *2.1 Compass alignment*

The compass alignment process is usually divided into two steps, firstly is horizontal leveling and then is azimuth alignment. The azimuth alignment is performed on the basis of the horizontal leveling, and the compass azimuth alignment method is generally adopted.

(1) Horizontal alignment

After the SINS is coarsely aligned, the misalignment angle can be regarded as a small angle, so the intersection of the horizontal misalignment angle $\phi_E$ and $\phi_N$ can be neglected during the fine alignment process. Fig. 1 shows the northward alignment channel of the SINS compass alignment loop.

The relationship between input and output of the third-order alignment loop is as follows [Qin (2014)]:

$$\phi_E(s)=\frac{(s+K_1)}{\Delta_3(s)}(\varepsilon_E-\phi_U\omega_{ie}\cos L)-\frac{\left(\frac{1+K_2}{R}+\frac{K_3}{s}\right)}{\Delta_3(s)}\nabla_N \tag{1}$$

where, $\Delta_3(s)=s^3+K_1s^2+(1+K_2)\omega_s^2+gK_3$, $K_1$, $K_2$ and $K_3$ are compass loop parameters.

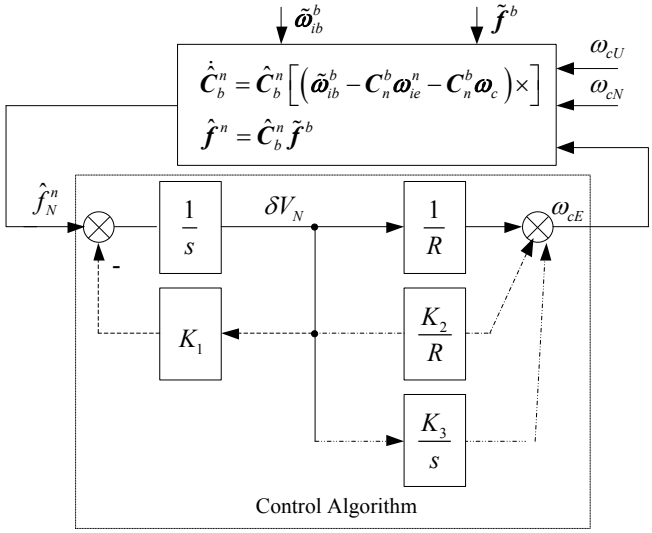


**Figure 1:** The north channel of the horizontal alignment for SINS

(2) Azimuth alignment

Fig. 2 shows the SINS azimuth alignment loop. After the horizontal alignment, the horizontal misalignment angle can reach the angular second level, and the velocity error caused by the horizontal misalignment angle can be neglected.

Take $K(s)=K_3/\left(\omega_{ie}\cos L(s+K_4)\right)$, the relationship between input and output of the above azimuth alignment loop is as follows [Qin (2014)]

$$\begin{aligned}\phi_U(s)=&\frac{sK(s)}{\Delta^*(s)}\left[\frac{\nabla_N(s)}{s}+\delta V_N(0)\right]+\frac{gK(s)}{\Delta^*(s)}\left[\frac{\varepsilon_E(s)}{s}+\phi_E(0)\right]\\&+\frac{s(s+K_1)+\frac{K_2+1}{R}g}{\Delta^*(s)}\left[\frac{\varepsilon_U}{s}+\phi_U(0)\right]\end{aligned} \tag{2}$$

where, $\Delta^*(s) = s^3 + k_1 s^2 + \omega_s^2 \left(K_2 + 1\right) s + \left(K_3 / (s + K_4)\right) g$ , $K_1$ , $K_2$ , $K_3$ and $K_4$ are compass loop parameters.

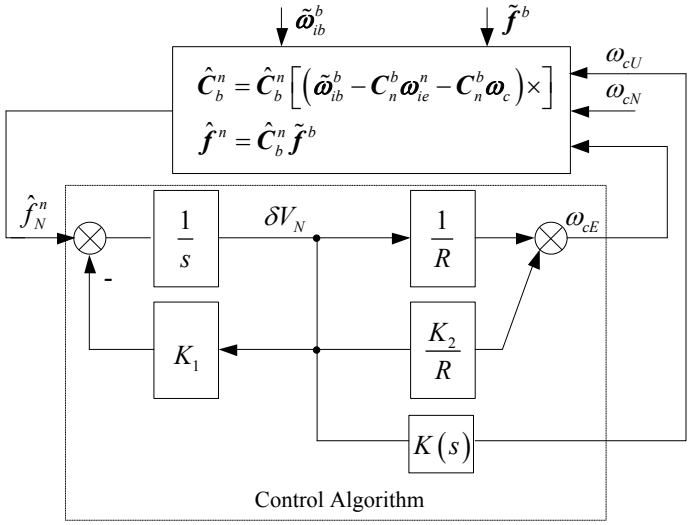


**Figure 2:** The north channel of the horizontal alignment for SINS

### *2.2 Forward navigation algorithm*

In this paper, the "Northward-Eastward-Upward (ENU)" geographic coordinate system is selected as the navigation coordinate system, which is recorded as $n$ coordinate system, and the "Right-Front-Upward (RFU)" coordinate system is selected as the body coordinate system, which is recorded as $b$ coordinate system.

The attitude, velocity and position navigation algorithms of SINS can be expressed by the following set of differential equations [Deng, Sun, Ding et al. (2019); Zhang, Wang, Jin et al. (2019)]:

$$\dot{\boldsymbol{C}}_b^n = \boldsymbol{C}_b^n \left( \boldsymbol{\omega}_{nb}^b \times \right) \tag{3}$$

$$\dot{\boldsymbol{V}}^n = \boldsymbol{C}_b^n \boldsymbol{f}^b - \left( 2\boldsymbol{\omega}_{ie}^n + \boldsymbol{\omega}_{en}^n \right) \times \boldsymbol{V}^n + \boldsymbol{g}^n \tag{4}$$

$$\dot{L} = \frac{V_N^n}{R}, \dot{\lambda} = \frac{V_E^n \sec L}{R} \tag{5}$$

where, $\boldsymbol{\omega}_{nb}^b = \boldsymbol{\omega}_{ib}^b - (\boldsymbol{C}_b^n)^T (\boldsymbol{\omega}_{ie}^n + \boldsymbol{\omega}_{en}^n)$ , $\boldsymbol{\omega}_{en}^n = [-V_N^n / R \quad V_E^n / R \quad V_E^n \tan L / R]^T$ ; the symbol $\boldsymbol{A}_{BC}^D$ represents the projection of a motion vector $\mathbf{A}$ which the coordinate system $C$ relative to the coordinate system $B$ in the coordinate system $D$ , $\boldsymbol{C}_b^n$ is attitude matrix, $\boldsymbol{V}^n = [V_E^n \quad V_N^n \quad V_U^n]^T$ is velocity vector in the navigation coordinate system $n$ , $L$ and $\lambda$ are the latitude and longitude respectively, $\boldsymbol{\omega}_{ib}^b$ and $\boldsymbol{f}^b$ denote angular velocity measurement of gyro and accelerometer measurement respectively, $\boldsymbol{\omega}_{ie}$ and $\mathrm{g}$ are angular rate of the Earth's rotation and the local acceleration, $R$ is Earth radius, and $(\bullet\times)$ represents antisymmetric matrix of the vector $\bullet$ .

In order to facilitate the processing of the computer, the Eqs. (1)-(3) need to be discretized. When the carrier is generally maneuverable, a single-subsample algorithm can be used, namely, only one inertial instrument data acquisition is performed in one navigation calculation update cycle. Assuming the navigation calculation cycle and the instrument data sampling period are both $T_s$, the discrete form of the basic equation of the navigation calculation can be expressed as follows:

$$\boldsymbol{C}_{bk}^{n} = \boldsymbol{C}_{bk-1}^{n}\left(\boldsymbol{I} + T_s\boldsymbol{\omega}_{nbk}^{b}\times\right) \tag{6}$$

$$\boldsymbol{V}_{k}^{n} = \boldsymbol{V}_{k-1}^{n} + T_s\left[\boldsymbol{C}_{bk-1}^{n}\boldsymbol{f}_{k-1}^{b} - \left(2\boldsymbol{\omega}_{iek-1}^{n} + \boldsymbol{\omega}_{enk-1}^{n}\right)\times\boldsymbol{V}_{k-1}^{n} + \boldsymbol{g}^{n}\right] \tag{7}$$

$$L_k = L_{k-1} + \frac{T_s V_{Nk-1}^{n}}{R}, \lambda_k = \lambda_{k-1} + \frac{T_s V_{Ek-1}^{n}\sec L_{k-1}}{R} \tag{8}$$

where, $k$ is the navigation updating times, $\boldsymbol{\omega}_{nbk}^{b} = \boldsymbol{\omega}_{ibk}^{b} - (\boldsymbol{C}_{bk-1}^{n})^{T}(\boldsymbol{\omega}_{iek-1}^{n} + \boldsymbol{\omega}_{enk-1}^{n})$ , $\boldsymbol{\omega}_{iek}^{n} = [0 \quad \omega_{ie}\cos L_k \quad \omega_{ie}\sin L_k]^{T}$ , $\boldsymbol{\omega}_{enk}^{n} = [-V_{Nk}^{n}/R \quad V_{Ek}^{n}/R \quad V_{Ek}^{n}\tan L_k/R]^{T}$ , $(k = 1,2,3\cdots)$ .

### *2.3 Reverse navigation algorithm*

Assuming that from $t_0$ to $t_m$, the SINS navigates from point A to point B. In order to make the software algorithm navigate backward from point B to point A, the Eqs. (6)-(8) are shifted and slightly changed, then the SINS reverse algorithm is as follows:

$$\boldsymbol{C}_{bk-1}^{n} = \boldsymbol{C}_{bk}^{n}\left(\mathbf{I} + T_s\boldsymbol{\omega}_{nbk}^{b}\times\right)^{-1} \approx \boldsymbol{C}_{bk}^{n}\left(\mathbf{I} - T_s\boldsymbol{\omega}_{nbk}^{b}\times\right) \approx \boldsymbol{C}_{bk}^{n}\left(\mathbf{I} - T_s\boldsymbol{\omega}_{nbk-1}^{b}\times\right) \tag{9}$$

$$\begin{aligned}\boldsymbol{V}_{k-1}^{n} &= \boldsymbol{V}_{k}^{n} - T_s\left[\boldsymbol{C}_{bk-1}^{n}\boldsymbol{f}_{k-1}^{b} - \left(2\boldsymbol{\omega}_{iek-1}^{n} + \boldsymbol{\omega}_{enk-1}^{n}\right)\times\boldsymbol{V}_{k-1}^{n} + \boldsymbol{g}^{n}\right] \\ &\approx \boldsymbol{V}_{k}^{n} - T_s\left[\boldsymbol{C}_{bk}^{n}\boldsymbol{f}_{k}^{b} - \left(2\boldsymbol{\omega}_{iek}^{n} + \boldsymbol{\omega}_{enk}^{n}\right)\times\boldsymbol{V}_{k}^{n} + \boldsymbol{g}^{n}\right]\end{aligned} \tag{10}$$

$$\begin{cases} L_{k-1} = L_k - \dfrac{T_s V_{Nk-1}^{n}}{R} \approx L_k - \dfrac{T_s V_{Nk}^{n}}{R} \\ \lambda_{k-1} = \lambda_k - \dfrac{T_s V_{Ek-1}^{n}\sec L_{k-1}}{R} \approx \lambda_k - \dfrac{T_s V_{Ek}^{n}\sec L_k}{R} \end{cases} \tag{11}$$

If remember that $\hat{\boldsymbol{C}}_{bm-j}^{n} = \boldsymbol{C}_{bj}^{n}$ , $\hat{\boldsymbol{V}}_{m-j}^{n} = -\boldsymbol{V}_{j}^{n}$ , $\hat{L}_{m-j} = L_j$ , $\hat{\lambda}_{m-j} = \lambda_j$ , $\hat{\boldsymbol{\omega}}_{ibm-j}^{b} = -\boldsymbol{\omega}_{ibj}^{b}$ , $\hat{\boldsymbol{f}}_{m-j}^{b} = \boldsymbol{f}_{sf}^{b}$ , $\hat{\boldsymbol{\omega}}_{iem-j}^{n} = -\boldsymbol{\omega}_{iej}^{n}$ , $\hat{\boldsymbol{\omega}}_{nbm-j}^{b} = \boldsymbol{\omega}_{nbj}^{b}$ , $\hat{\boldsymbol{\omega}}_{ie}^{n} = -\boldsymbol{\omega}_{ie}^{n}$ , $(j = 0,1,2\cdots m)$ and make $p = m - k + 1$ , then convert by token and subscript, such as $\boldsymbol{C}_{bk-1}^{n} = \boldsymbol{C}_{bm-p}^{n} = \hat{\boldsymbol{C}}_{bp}^{n}$ and $\boldsymbol{C}_{bk}^{n} = \boldsymbol{C}_{bm+1-p}^{n} = \hat{\boldsymbol{C}}_{bp-1}^{n}$, and so on, Eqs. (9)-(11) can be described as follows:

$$\hat{\boldsymbol{C}}_{bp}^{n} = \hat{\boldsymbol{C}}_{bp-1}^{n}\left(\boldsymbol{I} + T_s\hat{\boldsymbol{\omega}}_{nbp}^{b}\times\right) \tag{12}$$

$$\hat{\boldsymbol{V}}_{p}^{n} = \hat{\boldsymbol{V}}_{p-1}^{n} + T_s\left[\hat{\boldsymbol{C}}_{bp-1}^{n}\hat{\boldsymbol{f}}_{p}^{b} - \left(2\hat{\boldsymbol{\omega}}_{iep-1}^{n} + \hat{\boldsymbol{\omega}}_{enp-1}^{n}\right)\times\hat{\boldsymbol{V}}_{p-1}^{n} + \boldsymbol{g}^{n}\right] \tag{13}$$

$$\begin{cases} \hat{L}_p = \hat{L}_{p-1} + \dfrac{T_s\hat{V}_{Np-1}^{n}}{R} \\ \hat{\lambda}_p = \hat{\lambda}_{p-1} + \dfrac{T_s\hat{V}_{Ep-1}^{n}\sec\hat{L}_{p-1}}{R} \end{cases} \tag{14}$$

where, $\hat{\boldsymbol{\omega}}_{iep}^{n}=-\boldsymbol{\omega}_{iem-p}^{n}=-[0 \quad \omega_{ie}\cos L_{m-p} \quad \omega_{ie}\sin L_{m-p}]^{T}=[0 \quad \hat{\omega}_{ie}\cos \hat{L}_{p} \quad \hat{\omega}_{ie}\sin \hat{L}_{p}]^{T}$,

$\hat{\boldsymbol{\omega}}_{enp}^{n}=-\boldsymbol{\omega}_{enm-p}^{n}=-[-V_{Nm-p}^{n}/R \quad V_{Em-p}^{n}/R \quad V_{Em-p}^{n}\tan L_{m-p}/R]^{T}=-[-\hat{V}_{Np}^{n}/R \quad \hat{V}_{Ep}^{n}/R \quad \hat{V}_{Ep}^{n}\tan L_{p}/R]^{T}$

, $\hat{\boldsymbol{\omega}}_{nbp}^{b}=\boldsymbol{\omega}_{nbm-p}^{b}=-[\boldsymbol{\omega}_{ibm-p}^{b}-(\boldsymbol{C}_{bm-p+1}^{n})^{T}(\boldsymbol{\omega}_{iem-p+1}^{n}+\boldsymbol{\omega}_{enm-p+1}^{n})]=\hat{\boldsymbol{\omega}}_{ibp}^{b}-(\hat{\boldsymbol{C}}_{bp+1}^{n})^{T}(\hat{\boldsymbol{\omega}}_{iep+1}^{n}+\hat{\boldsymbol{\omega}}_{enp-1}^{n})$.

By comparing Eqs. (9)-(11) and Eqs. (12)-(14), it is found that they are completely consistent in the form of the algorithm. It can be seen from the above analysis that if only the symbol of gyroscope sampling and the Earth rotation angle rate in the forward algorithm are reversed, and the initial value of the reverse navigation algorithm is set as follows: $\hat{\boldsymbol{C}}_{b0}^{n}=\boldsymbol{C}_{bm}^{n}, \hat{\boldsymbol{V}}_{0}^{n}=-\boldsymbol{V}_{m}^{n}, \hat{L}_{0}=L_{m}, \hat{\lambda}_{0}=\lambda_{m}$, the sampling data are reversed processed. Then the inverse navigation calculation from moment (point B) to moment (point A) can be realized. It is not difficult to find that in the process of forward and reverse navigation, if the calculation error is not considered, the attitude matrix and position coordinates of the two processes are equal at the same time of the data sequence, while the magnitude of velocity is equal but the sign is opposite. It is worth pointing out that quaternion, equivalent rotation vector and cone motion compensation should be used to reduce the algorithm error in practical application of SINS calculation, but similar reverse algorithms and conclusions can be obtained.

## 3 Simulations and analysis

### *3.1 Parameter settings of the compass alignment for SINS*

(1) Parameter setting of the horizontal alignment loop

It can be known from Eqs. (1) and (2) that the alignment accuracy of the three-order horizontal alignment loop is independent of $K_1, K_2, K_3$, and so only the influence on the dynamic performance of the system can be considered when $K_1, K_2, K_3$ are set.

If the attenuation coefficient of the alignment loop is $\sigma$, and the damping oscillation frequency is $\omega_d$, then the eigenvalues of the three-order system are as follows:

$$s_1=-\sigma, s_2=-\sigma+j\omega_d, s_3=-\sigma-j\omega_d \tag{15}$$

So the characteristic polynomial is

$$\Delta_3(s)=(s+\sigma)(s+\sigma-j\omega_d)(s+\sigma+j\omega_d)=s^3+3\sigma s^2+(3\sigma^2+\omega_d^2)s+\sigma^3+\sigma\omega_d^2 \tag{16}$$

It can be obtained through comparing Eq. (1) with Eq. (16)

$$\begin{cases} K_1=3\sigma \\ K_2=(3\sigma^2+\omega_d^2)/\omega_s^2-1 \\ K_3=(\sigma^3+\sigma\omega_d^2)/g \end{cases} \tag{17}$$

Assume that the required damping ratio of the system is $\xi$, the attenuation coefficient is $\sigma$, then [Gao, Lu and Yu (2015)]

$$\begin{cases} K_1=3\sigma \\ K_2=(2+1/\xi^2)\sigma^2/\omega_s^2-1 \\ K_3=\sigma^3/g\xi^2 \end{cases} \tag{18}$$

where, $\sigma = \dfrac{2\pi\xi}{T_{xy}\sqrt{1-\xi^2}}$, $T_{xy}$ is horizontal control loop period.

(2) Parameter setting of the azimuth alignment loop

In the azimuth alignment loop of the compass method, a two-order fast horizontal alignment loop is adopted in the northward channel, but the parameters of $K_1$ and $K_2$ in the loops are not the same as those in the horizontal alignment, and must be determined separately.

According to the dynamic response requirements, the damping ratio is set as $\xi = \sqrt{2}/2$, the attenuation coefficient is $\sigma$, then the damping oscillation frequency is $\omega_d = \sigma$, so the eigenvalue are as follows:

$$s_{1,2} = -\sigma - j\sigma \text{ , } s_{3,4} = -\sigma + j\sigma \tag{19}$$

$$\Delta(s) = [(s+\sigma+j\sigma)(s+\sigma-j\sigma)]^2 = s^4 + 4\sigma s^3 + 8\sigma^2 s^2 + 8\sigma^3 s + 4\sigma^4 \tag{20}$$

According to Eq. (2), the characteristic polynomial of the azimuth alignment loop is

$$\begin{aligned}\Delta(s) &= s^3(s+K_4) + K_1 s^2(s+K_4) + \omega_s^2(K_2+1)s(s+K_4) + gK_3 \\ &= s^4 + (K_1+K_4)s^3 + [\omega_s^2(K_2+1) + K_1K_4]s^2 + \omega_s^2(K_2+1)K_4 s + gK_3\end{aligned} \tag{21}$$

It can be gotten through comparing Eq. (20) with Eq. (21):

$$\begin{cases} K_1 + K_4 = 4\sigma \\ \omega_s^2(K_2+1) + K_1K_4 = 8\sigma^2 \\ \omega_s^2(K_2+1)K_4 = 8\sigma^2 \\ gK_3 = 4\sigma^4 \end{cases} \tag{22}$$

Eq. (22) is a nonlinear equation set with unknown parameters, and there are multiple calculations. If $K_1 = K_4$, then a unique calculation is obtained [Gao, Lu and Yu (2015)]:

$$\begin{cases} K_1 = K_4 = 2\sigma \\ K_2 = 4\sigma^2/\omega_S^2 - 1 \\ K_3 = 4\sigma^4/g \end{cases} \tag{23}$$

where, $\sigma = \dfrac{2\pi\xi}{T_z\sqrt{1-\xi^2}} \approx \dfrac{2\pi}{T_z}$, $T_z$ is convergence period of the azimuth alignment loop.

Because $\sigma$ is proportional to the convergence speed of the system, and it is inversely proportional to the anti-interference ability of the system. During the course of the azimuth alignment of the compass method, the convergence speed of the system can be adjusted in a manner of changing $\sigma$. In the initial stage of the azimuth alignment, a larger value of $\sigma$ can be selected to increase the convergence speed of the system.

$\xi = \sqrt{2}/2 \approx 0.707$ is selected as damping coefficient, the adjustment time of the horizontal and azimuth alignment loop are selected for 150 s and 450 s, respectively. Therefore, the parameter of the horizontal fine alignment loop is calculated as $K_1 = 0.06$, $K_2 = 1040.33306122$, $K_3 = 0.000081632653$; the parameter of the azimuth fine alignment is $K_1 = K_4 = 0.02$, $K_2 = 259.3332653$, $K_3 = 4.082\text{e-}9$.

### *3.2 Simulation experiment of fast compass alignment method*

(1) Simulation experiment conditions

Gyro: Constant drift is $0.02^\circ / h$, Random drift is $0.006^\circ / h$;

Accelerometer: Constant bias is $50\mu g$, Random bias is $50\mu g$;

Longitude: 118.786365°;

Latitude: 32.057313°;

Data sampling frequency: 200 Hz;

Calculation period: 5 ms;

Initial attitude: Pitch, roll and heading are all 0°;

Initial attitude error: Pitch and roll are both 0.1°, Heading is 1.5°;

Simulation time: 600 s.

(2) Simulation experiment of static base

In the case of static base, two alignment methods are compared through simulation: 1) compass alignment based on normal navigation calculation (Scheme 1); 2) compass alignment based on the first 80 s of stored data and repeated navigation calculation (Scheme 2); The attitude error curves based on Scheme 1 and Scheme 2 are shown in Fig. 3 and 4, respectively.

In Fig. 3, the horizontal coordinate axis parameter is shown as alignment (or simulation) time for Scheme 1; in Fig. 4 the horizontal coordinate axis parameter is iterative update times ($t \times 200$) for Scheme 2.

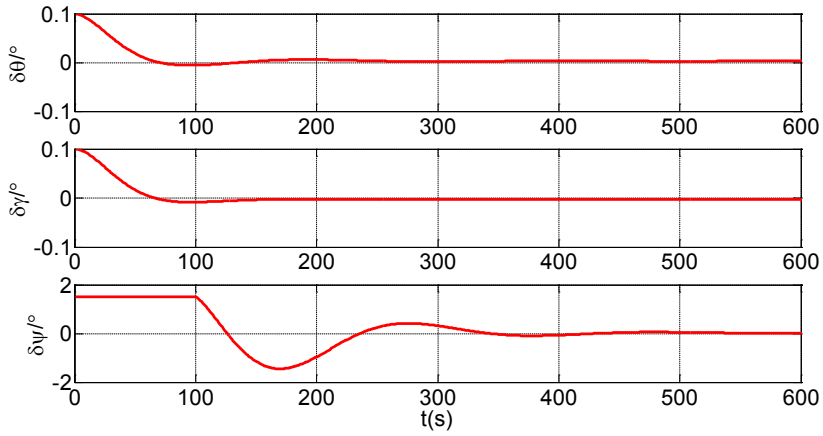


**Figure 3:** Compass alignment error curve based on the normal navigation calculation of static base

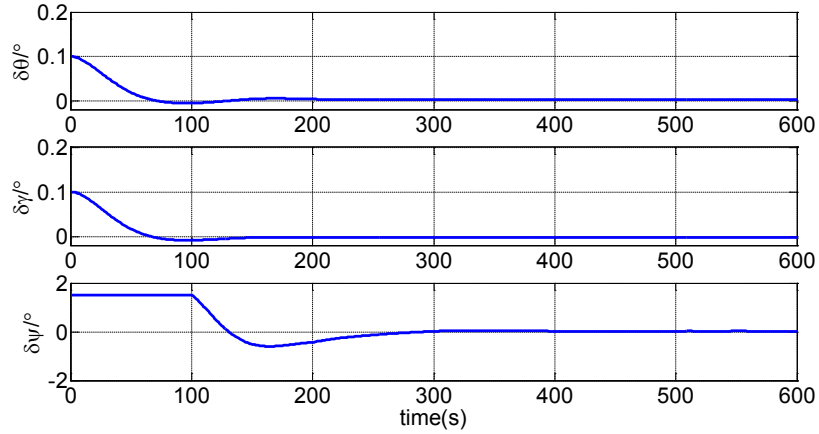


**Figure 4:** Compass alignment error curve based on the first 80 s of stored data and repeated navigation calculation of static base

As shown in Figs. 3 and 4, both the Schemes 1 and 2 have completed the initial alignment, and the attitude error curves can converge to near 0; the data of fully stabilized for 550~600 in the alignment error curve is collected, and the statistics results are shown in Tab. 1 and it shows that the alignment based on the stored data and the repeated navigation calculation can effectively complete the initial alignment, and can achieve the accuracy of the classic compass method.

**Table 1:** Statistics results of two schemes under static base

| Error | Scheme 1 | Scheme 2 |
|---|---|---|
| Pitch (°) | 0.00261 | 0.00234 |
| Rolling (°) | -0.00208 | -0.00209 |
| Heading (°) | 0.0251 | 0.0236 |

(3) Simulation experiment of swing base

The model of ship's three-axis rocking motion is as follows [Xu, He, Qin et al. (2017)]:

$$\begin{cases} \theta = A_\theta \sin(\omega_\theta t + \phi_\theta) \\ \gamma = A_\gamma \sin(\omega_\gamma t + \phi_\gamma) \\ \varphi = A_\varphi \sin(\omega_\varphi t + \phi_\varphi) \end{cases} \tag{24}$$

The pitch swing amplitude $A_\theta$=8°, the swing frequency $\omega_\theta$=0.15 Hz; the rolling swing amplitude $A_\gamma = 6^\circ$, the swing frequency $\omega_\gamma$=0.2 Hz; the heading swing amplitude $A_\varphi = 5^\circ$ and the swing frequency $\omega_\varphi$=0.125 Hz. The swing centers of pitch, roll and heading are all set to $0^\circ$. Attitude error curves based on Schemes 1 and 2 are shown in Figs. 5 and 6, respectively. In Fig. 5, the horizontal coordinate axis parameter is shown as alignment (or simulation) time for Scheme 1; in Fig. 6 the horizontal coordinate axis parameter is iterative update times ($t \times 200$) for Scheme 2.

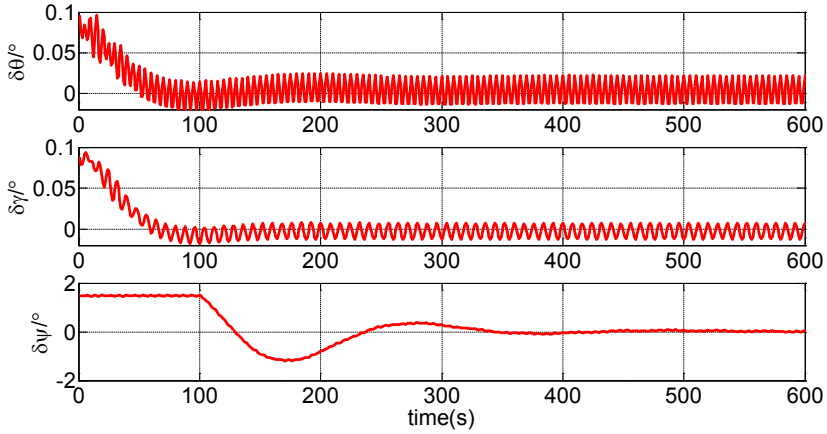


**Figure 5:** Compass alignment error curve based on the normal navigation calculation of swing base

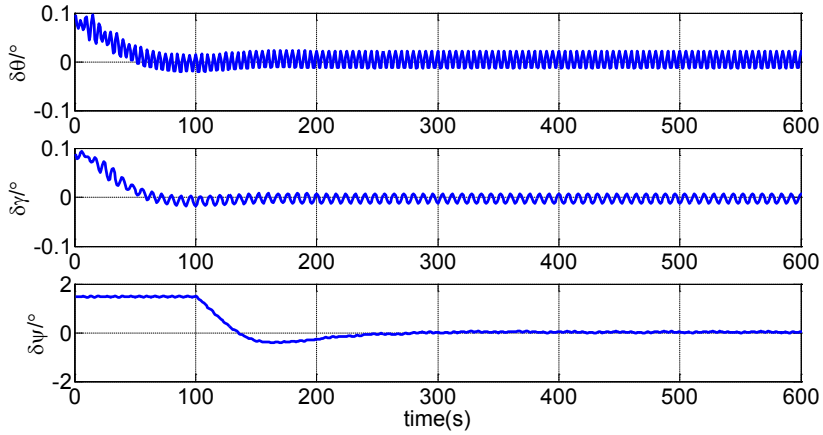


**Figure 6:** Compass alignment error curve based on the first 80 s of stored data and repeated navigation calculation of swing base

**Table 2:** Statistics results of two schemes under swing base

| Error | Scheme 1 | Scheme 2 |
|---|---|---|
| Pitch (°) | 0.00261 | 0.00234 |
| Rolling (°) | -0.00208 | -0.00209 |
| Heading (°) | 0.0251 | 0.0236 |

As shown in Figs. 5 and 6, both the Schemes 1 and 2 have completed the initial alignment, and the attitude error curves can converge to near 0; the data of fully stabilized for 550~600 in the alignment error curve is collected, and the statistics results are shown in Tab. 2, and it shows that the alignment based on the stored data and the repeated navigation calculation can effectively complete the initial alignment, and can achieve the accuracy of the classic compass method.

## 4 Conclusion

This paper deduces the reverse navigation algorithm in more detail. In the azimuth alignment of the compass alignment method, the larger initial azimuth error angle generally leads to more oscillations during the azimuth convergence of the compass alignment, but the alignment accuracy often depends only on the oscillation convergence accuracy of the later period. Therefore, if the reverse navigation algorithm is used, the diversity of SINS mathematics platform can also use the same sampling data sequence in the early and late stages of the compass azimuth alignment. Firstly, the initial azimuth error processing is reduced, and then the accuracy-determined azimuth alignment is performed, which is beneficial to further shorten the initial alignment time. The simulation experiment was done. In summary, when the computer performance is sufficiently high, the compass alignment method based on the stored data and the forward and reverse navigation calculation can effectively improve the alignment speed and improve the alignment accuracy.

**Funding Statement:** This work was supported by the National Nature Science Foundation of China (Grant No. 5200110367); Natural Science Foundation of Jiangsu Province (Grant No. SBK2020043219); Scientific Research Foundation of the Higher Education Institutions of Jiangsu Province (Grant No. 19KJB510052); NUPTSF (Grant No. NY219023).

**Conflicts of Interest:** The authors declare that they have no conflicts of interest to report regarding the present study.

## References

**Chang, L. B.; Hu, B. Q.; Li, Y.** (2015): Backtracking integration for fast attitude determination-based initial alignment. *IEEE Transactions on Instrumentation and Measurement*, vol. 64, no. 3, pp. 795-803.

**Chang, L. L.; Qin, F. J.; Li, A**. (2015): A novel backtracking scheme for attitude determination-based initial alignment. *IEEE Transactions on Automation Science and Engineering*, vol. 12, no. 1, pp. 384-390.

**Deng, Z. L.; Sun, J.; Ding, F.; Ismail, M. W. M.** (2019): a novel damping method for strapdown inertial navigation system. *IEEE Access*, vol. 7, pp. 49549-49557.

**Gao, W.; Lu, B. F.; Yu, C. Y.** (2015): Forward and backward processes for INS compass alignment. *Ocean Engineering*, vol. 98, pp. 1-9.

**Hao, Y. L.; Zhang, Y.; Sun, F.** (2011): Research of gyro-compassing alignment for large azimuth misalignment. *Chinese Journal of Scientific Instrument*, vol. 32, no. 7, pp. 1478-1484.

**Li, W. L.; Wu, W. Q.; Wang, J. L.; Lu, L. Q.** (2012): A fast SINS initial alignment scheme for underwater vehicle applications. *Journal of Navigation*, vol. 66, no. 2, pp. 181-198.

**Li, Y.; Xu, X. S.; Wu, B. X.** (2008): Gyrocompass self-alignment of SINS. *Journal of Chinese Inertial Technology*, vol. 16, no. 4, pp. 386-389.

**Liu, X. X.; Xu, X. S.; Wang, L. H.; Liu, Y.T.** (2013): A fast compass alignment method for SINS based on saved data and repeated navigation solution. *Measurement*, vol. 2013, no. 46, pp. 3836-3846.

**Liu, Y. T.; Xu, X. S.; Zhang, T.; Wu, L.; Sun, J. et al.** (2015): Compassing alignment in motion based on external reference velocity. *Journal of Chinese Inertial Technology*, vol. 2, pp. 165-171.

**Qin, Y. Y.** (2014): *Inertial Navigation-2nd Edition*. Science Press.

**Ren, Y. J.; Liu, Y. P.; Ji, S.; Sangaiah, A. K.; Wang, J.** (2018): Incentive mechanism of data storage based on blockchain for wireless sensor networks. *Mobile Information Systems*, vol. 2018, pp. 1-10.

**Sun, Y. D.; Wang, L. F.; Cai, Q. Z.; Yang, G. L.; Wen, Z. Y.** (2019): In-motion attitude and position alignment for odometer-aided SINS based on backtracking scheme. *IEEE Access*, vol. 7, pp. 20211-20224.

**Wang, J.; Zhang, T.; Tong, J. W.; Li, Y.** (2020): A fast SINS self-alignment method under geographic latitude uncertainty. *IEEE Sensors Journal*, vol. 20, no. 6, pp. 2885-2894.

**Xu, J. N.; He, H. Y.; Qin, F. J.; Chang, L. B.** (2017): A novel autonomous initial alignment method for strapdown inertial navigation system. *IEEE Transactions on Instrumentation and Measurement*, vol. 66, no. 9, pp. 2274-2282.

**Zhang, T.; Wang, J.; Jin, B. N.; Li, Y.** (2019): Application of improved fifth-degree cubature Kalman filter in the nonlinear initial alignment of strapdown inertial navigation system. *Review of Scientific Instruments*, vol. 90, no. 1, pp. 1-15.